Food Chemistry 286 (2019) 87–97

Contents lists available at ScienceDirect

Food Chemistry

journal homepage: www.elsevier.com/locate/foodchem

Research Article

Metabolomic analysis of energy regulated germination and sprouting of organic mung bean (*Vigna radiata*) using NMR spectroscopy

Lin Chen[a,c], Ji'en Wu[b], Zhanming Li[a], Qin Liu[a,c], Xue Zhao[a,c], Hongshun Yang[a,c,*]

[a] Food Science and Technology Programme, c/o Department of Chemistry, National University of Singapore, Singapore 117543, Singapore
[b] The Nuclear Magnetic Resonance Laboratory, Department of Chemistry, National University of Singapore, Singapore 117543, Singapore
[c] National University of Singapore (Suzhou) Research Institute, 377 Lin Quan Street, Suzhou Industrial Park, Suzhou, Jiangsu 215123, PR China

ARTICLE INFO

Keywords:
Vegetable
ATP
Metabolomics
Principal component analysis
Organic produce
Transcriptional expression
Organic food
Omics

ABSTRACT

Germination and sprouting are regulated by the energy status. In the present study, mung bean seeds were treated with adenosine triphosphate and 2,4-dinitrophenol (DNP). The metabolomic changes during development of mung beans under different energy statuses were investigated. In total, 42 metabolites were identified. Principal component analysis revealed that the featured compounds produced in seeds were oleic, linoleic, and succinic acids. Sugars, including maltose, sucrose, and glucose were related to sprouting. Mung bean seeds utilised diverse energy resources and produced higher succinic acid content. Sugars and secondary metabolites accumulated in sprouts. Nitrogen, sugar, and amino acid metabolism pathways contributed to this physiological process. DNP caused an energy deficit, which resulted in the consumption and translation of glucose. Higher contents of other saccharides and amino acids were observed. The transcriptional results further confirmed our metabolic hypothesis. In conclusion, sufficient energy supply is crucial for sprout development and nutritive metabolite synthesis.

1. Introduction

The consumption of ready-to-eat organic sprout products (mung bean, broccoli, radish, alfalfa, etc.) has continuously increased in recent decades because of their high nutrition and convenience (Chen, Tan, et al., 2018). During the germination and sprouting processes of edible seeds, complex physiological changes contribute to the increased nutritional values and reduced contents of antinutrients. For instance, higher contents of phenolics and flavonoids, which resulted in elevated antioxidant capacities, were recorded in germinated legumes compared with those in seeds (Aguilera et al., 2013; Duenas, Hernández, Estrella, & Fernández, 2009). In addition, the 8-day germination of flaxseeds led to enhanced contents of amino acids and ascorbic acid (Wang, Wang, et al., 2016). By contrast, the levels of non-nutritional components, including lectins, oil, linustatin, and trypsin inhibitors, were decreased after germination and sprouting. The synthesis of various bioactive factors helps to protect the seed from environmental stresses and promote development.

Energy metabolism plays an important role in the regulation of various vital activities in plants. The accumulation of energy by aerobic respiration is an early event of seed germination and the inchoate energy supply contributes to starting the life cycle (Zhang et al., 2017). During the germination process, the stored polysaccharides, lipids, and proteins are degraded and used as energy sources and developmental materials (Smiri, Chaoui, & El Ferjani, 2009). Recent studies have revealed that the energy status is closely related to the nutritive properties of pre/post-harvest fruit and vegetables. For postharvest crops, an energy deficit or low level of adenosine triphosphate (ATP) results in nutritive disorder and senescence (Wang et al., 2013). The vacuum infiltration of exogenous ATP (1 mM) into litchi fruits effectively improved the endocellular ATP level and energy charge. The phenolic contents and antioxidant activities were maintained, and the browning

Abbreviations: ATP, adenosine triphosphate; SnRK, sucrose nonfermenting-1-related kinase; NMR, nuclear magnetic resonance; 2D, two-dimensional; PCA, principal component analysis; OPLS-DA, orthogonal partial least squares discriminant analysis; PCR, polymerase chain reaction; DI, distilled; DNP, 2,4-dinitrophenol; HSQC, heteronuclear single quantum coherence spectroscopy; D_M, Mahalanobis distance; F_t, true F value; F_c, critical F value; VIP, variable importance in projection; KEGG, Kyoto Encyclopedia of Genes and Genomes; UGPU, UTP-glucose-1-phosphate uridylyltransferase; FB, fructose-1,6-bisphosphatase; PD, pyruvate dehydrogenase; CS, citrate synthase; KD, 2-ketoglutarate dehydrogenase; SD, succinate dehydrogenase; TCA, tricarboxylic acid; PC, principal component; PLS, partial least squares

* Corresponding author at: Food Science and Technology Programme, c/o Department of Chemistry, National University of Singapore, Singapore 117543, Singapore.
E-mail address: chmynghs@nus.edu.sg (H. Yang).

https://doi.org/10.1016/j.foodchem.2019.01.183
Received 25 September 2018; Received in revised form 21 January 2019; Accepted 31 January 2019
Available online 07 February 2019
0308-8146/

and pathogenic infection could be prevented by positive energy regulation (Yi et al., 2010). Furthermore, our previous work showed that the energy supply was crucial for the nutritive formation of pre-harvest broccoli sprouts by the feedback regulation via the sucrose non-fermenting-1-related kinase (SnRK) pathway (Chen, Tan, et al., 2018). However, because of the complicated physiological metabolism and energy regulation of germination process, the global metabolic response of energy-regulated germination of organic edible seeds remains unclear.

Emerging metabolomic techniques, such as liquid chromatography-tandem mass spectrometry and nuclear magnetic resonance (NMR) make it more feasible to obtain comprehensive profiles of metabolic changes during plant physiological activities. For example, the metabolic changes of okra during postharvest storage were studied using ^{1}H NMR (Liu, Yuan, et al., 2017). Moreover, postharvest senescence and related characteristic markers were revealed using NMR-based metabolomics analysis (Yuan et al., 2017). Indeed, the metabolic analysis of energy regulated germination and sprouting processes may provide new insights to actively regulate and improve the nutritive values of sprouts or seedling products.

The objective of this work was to study the overall metabolic changes during the germination and sprouting of organic mung bean (*Vigna radiata*) under different energy statuses using high resolution NMR spectroscopy. Mung bean sprouts are widely consumed as fresh salad or a common side dish in Asia and western countries. They are also widely applied as a health food, and in cosmetics and medications because of their abundant proteins, polypeptides, polysaccharides, and polyphenols (Tang, Dong, Ren, Li, & He, 2014). This work helps to clarify the global metabolomic changes during mung bean development. It also provides a new strategy to enhance sprout quality to meet the increasing demand of ingredients and extractable nutraceutical yields in sprouts by the food and pharmaceutical industries. In the present study, the extracted metabolites were identified using two-dimensional (2D) NMR spectra and the principal component analysis (PCA) was applied to screen the principal metabolites responsible for the responses to the different treatments. The pairwise comparisons were checked by orthogonal partial least squares discriminant analysis (OPLS-DA) and pathway analysis was further conducted. Lastly, the expression patterns of selected genes were checked using real-time polymerase chain reaction (qPCR) to verify the metabolic analysis.

2. Materials and methods

2.1. Plant materials, treatment, and cultivation

Organic mung bean seeds were purchased from a local seed company in Singapore (Quan Fa Organic Farm, Singapore) and the treatment and cultivation were conducted according to the method of Baenas, García-Viguera, and Moreno (2014) with minor modifications. Briefly, the mung bean seeds were soaked in 3% (v/v) sodium hypochlorite (Sigma-Aldrich, St. Louis, MO, USA) for 5 min and then washed using distilled (DI) water several times. The sterilised seeds were immersed in DI water at 25 °C for 12 h. After that, the rehydrated seeds were separated into three groups, each contained approximately 100 g of seeds. Based on the results of preliminary studies, the seeds were immersed in 200 mL DI water (control), ATP (1 mM), and DNP (2 mM, 2,4-dinitrophenol, a respiratory uncoupling agent which inhibits the production of ATP) solutions, respectively for 5 min. Both ATP and DNP were purchased from Sigma-Aldrich (St. Louis, MO, USA). The treated seeds were washed by DI water to remove the residual chemicals, evenly spread on the seedling raising plates (30 cm × 22 cm), and germinated for 6 days in the dark (25 °C). The DI water in the raising plates was refreshed daily. Furthermore, at the third and fifth days of germination, 20 mL solutions of each treatment were evenly sprayed on the raising plates. During germination, the seed and sprout samples were collected, cut, frozen, ground, freeze dried, and stored in liquid nitrogen at day 0 and 6. Lastly, four groups including rehydrated seeds at day 0 (I), DNP treated sprouts (II), DI water treated sprouts (III), and ATP treated sprouts (IV) were sampled.

2.2. Preparation of mung bean extracts

The mung bean seed and sprout samples were weighed (50 mg) and mixed with 1.5 mL methanol-d_4 (Cambridge Isotope Laboratories, Tewksbury, MA, USA) in reaction tubes (15 mL). The mixtures were extracted in a water bath (40 °C) with continuous shaking for 30 min. After cooling to room temperature, the extracts were centrifuged at 12,000*g* at 4 °C for 20 min. The supernatants were collected and 600 μL of the methanol extract was transferred into a 5 mm magnetic tube (Sigma-Aldrich) and immediately subject to NMR analysis. All the experiments were conducted in triplicate (Yuan et al., 2017).

2.3. NMR spectroscopy analysis

All the prepared tubes were tested on a Bruker DRX-500 NMR spectrometer (Bruker, Rheinstetten, Germany) at a frequency of 500.23 MHz via a Triple Inverse Gradient probe, with a probe temperature of 25 °C (Liu, Wu, et al., 2017). The ^{1}H spectrum (metabolic profile) of each sample was collected using a first increment of the standard Bruker NOESY pulse sequence (noesypr1d). All the data were obtained using a spectral width of 20.0 ppm with an acquisition time of 3.3 s. Furthermore, the spectrum was recorded using 128 scans, 4 dummy scans, and a relaxation delay of 2 s. The 90° pulse length was modified for each sample using an automatic pulse calculation experiment (pulsecal) in TopSpin 3.6.0 (Bruker Rheinstetten, Germany). All free induction decays were multiplied by an exponential function equivalent to a 1-Hz line broadening factor before Fourier transformation. For signal assignment, standard 2D ^{1}H–^{13}C heteronuclear single quantum coherence spectroscopy (HSQC) of a representative sprout sample (day 6) was acquired at 25 °C using the Bruker hsqcedetgpsisp2.3 pulse sequence. The ^{1}H was recorded in the F2 channel with a 10.0 ppm spectrum width and ^{13}C was tested in the F1 channel with a 180.0 ppm spectrum width.

2.4. Spectral processing and statistical analysis

The resulting NMR spectrum of each sample was manually corrected for the phase and baseline distortions using the software TopSpin 3.6.0 (Bruker, Rheinstetten, Germany). The metabolites corresponding to the peaks were identified by 1D ^{1}H and 2D ^{1}H–^{13}C NMR spectra using the Madison Metabolomics Consortium Database (http://mmcd.nmrfam.wisc.edu), ChenomX NMR Suite (ChenomX Inc., Edmonton, AB, Canada), Biological Magnetic Resonance Data Bank (http://www.bmrb.wisc.edu/ metabolomics), PubChem database (https://pubchem.ncbi.nlm.nih.gov), and related references. Furthermore, the data were normalised to sum intensities and the region buckets with a width of 0.02 ppm were divided from normalised ^{1}H spectrum ranging from 0.5 to 10.0 ppm using the software Mestrenova (Mestreab Research SL, Santiago de Compostela, Spain). The water (4.80–4.90 ppm) and methanol (3.29–3.32 ppm) regions were excluded and the obtained standardised binned data was subject to multivariate analysis (Mahmud, Kousik, Hassell, Chowdhury, & Boroujerdi, 2015).

The dataset was built and imported into the SIMCA software (version 13.0, Umetrics, Sweden) and then PCA of the bucket tables was performed (Vong, Hua, & Liu, 2018). For the generated score plots, the Mahalanobis distance (D_M), two-sample Hotelling's T^2 test (T^2), true F value (F_t), and critical F value (F_c) were calculated using SPSS (IBM, Armonk, NY, USA) and MatLabR2013b (MathWork, Natick, MA, USA). The binned data were further analysed using OPLS-DA. The qualities of the models were verified using the R^2X and Q^2 values, which represented the explained variables and model predictability, respectively. Colour coded visualised loading and coefficient plots were

checked to illustrate the variables of metabolites that were associated with the energy regulated germination process. The colour-coded lines indicated the weights of the discriminatory variables and as the correlation coefficient gradually increased from 0 to 1, the colour changed from blue to red. Thus, it presented the resonance importance for the metabolic profile discrimination of pairwise groups. In addition, variable importance in projection (VIP) analysis was conducted on the processed data using the standard algorithms in the OPLS-toolbox. Metabolites with a VIP value > 1 were recognised as the most influenced factors in the extracted OPLS models. Lastly, the related metabolic pathways were analysed using MetaboAnalyst 4.0 (http://www.metaboanalyst.ca/) and their contributions and further biological interpretations were discussed based on the Kyoto Encyclopedia of Genes and Genomes (KEGG) database (https://www.genome.jp/kegg/pathway.html) (Liu et al., 2018).

2.5. Expression analysis of selected genes using real-time PCR

Based on the pathway analysis results, six genes [UTP-glucose-1-phosphate uridylyltransferase (UGPU), fructose-1,6-bisphosphatase (FB), pyruvate dehydrogenase (PD), citrate synthase (CS), 2-ketoglutarate dehydrogenase (KD), and succinate dehydrogenase (SD)] involved in glycolysis and tricarboxylic acid (TCA) cycle were selected to conduct the real-time PCR (qPCR) (Avin-Wittenberg, Tzin, Angelovici, Less, & Galili, 2012). The selected genes in mung bean were obtained by comparing the *Arabidopsis* genes with the whole genome of mung bean in the GenBank database and the specific primers for the best-matched genes were designed using Primer 5 software (Premier Biosoft International, Palo Alto, CA, USA) and are listed in Table S1. The specificities of the primers were further checked using Primer Blast at NCBI (https://www.ncbi.nlm.nih.gov/). Mung bean total RNA was extracted using a Total RNA Mini-Pre Kit (Bio Basic, Ontario, Canada) and the concentration and quality of the extracted RNA were checked using a spectrophotometer (BioDrop, Biochrom, Cambridge, UK). After testing the RNA integrity by 1% (w/v) agarose gel electrophoresis, cDNA was synthesised using a First Strand cDNA Synthesis Kit (Promega Corporation, Madison, WI, USA). The *VrActin* gene (GenBank accession: XM_014661327; sense primer: 5′-CGTGTTTCCTTCTGTTGTTGG-3′; antisense primer: 5′-CCTCTTTCCCTTAGCCTTGTC-3′) was used as the housekeeping gene. The reaction conditions were the same as those used in our previous report and the relative expression of each gene was calculated by the $2^{-\Delta\Delta CT}$ [$\Delta C_T = C_{T,\ Target} - C_{T,\ actin}$; $\Delta\Delta CT = \Delta C_{T,\ treatment} - \Delta C_{T,\ control\ (0d)}$] method (Chen, Zhou, et al., 2018). The data were normalised by log10 transformation and utilised to construct a heatmap in HemI 1.0 (CUCKOO Workgroup, Wuhan, Hubei, China).

2.6. Statistical analysis

Data were statistically analysed using analysis of variance (ANOVA), and means were compared using the least significant difference (LSD) method to test the effect of energy regulation on mung bean germination and sprouting. Differences with $P < 0.05$ were considered significant.

3. Results

3.1. Identification and comparison of metabolites in mung beans

The metabolic comparisons of mung bean seeds and sprouts are shown in Fig. 1. The results presented the different detections of essential primary and secondary metabolites in mung bean seeds and sprouts. Multiple ^{1}H signals were recorded from 0.5 to 10.0 ppm. Moreover, most signals were located in the region around 3.0–5.5 ppm in the four groups. In mung bean seeds, some signal peaks in the region from 0.5 to 3.0 ppm were also measured. Compared with seeds, higher intensities of most ^{1}H signals were recorded in the sprout samples and some additional signals could be found in the region around 5.5–8.5 ppm.

Based on the chemical shifts of ^{1}H and the 2D ^{1}H–^{13}C NMR spectra, the representative metabolites in mung bean were identified. In total, 42 metabolites were assigned (Fig. 2) and the chemical shifts of ^{1}H and ^{13}C are listed in Table S2. Various chemicals, including sugars, amino acids, fatty acids, organic acids, and some other secondary metabolites were detected. In the region of 0.5–3.0 ppm, abundant amino acids (e.g. isoleucine, leucine, valine, and threonine) and some organic acids, such as lactic acid and succinic acid, were identified. Furthermore, various sugars, including glucose, fructose, maltose, galactose, sucrose, raffinose, and arabinose, were found in the region from 5.5 to 8.5 ppm. Some unsaturated fatty acids (e.g. linolenic acid, oleic acid, and linoleic acid) were also identified in this area. Moreover, in the region around 5.5–8.5 ppm, other bioactive components, such as indole-3-acetic acid, *P*-coumaric acid, vanillin, and trigonelline, were assigned (Fig. 2A).

3.2. Principal component analysis

PCA was conducted to screen the principle metabolites and highlight the metabolic changes during the energy-regulated germination of mung beans. The first two principal components (PCs) explained 95.7% of the total data obtained from the four treated groups and PC1 explained 90.9% (Fig. 3A). The results of the score plot clearly showed that the data from four groups were well separated into three clusters (Fig. 3B). Samples from the same group were aggregated and the metabolite profile from mung bean seeds (I) was mainly affected by PC1. The sprout groups (II–IV) were all negatively influenced by PC1, and the DNP treated group (II) was positively affected by PC2. Control (III) and ATP (IV) treated groups were clustered and negatively influenced by PC2.

A loading plot was used to monitor the distinct metabolites responsible for the variable separation (Fig. 3C). Metabolites such as oleic acid, betaine, linoleic acid, succinic acid, phenylalanine, glucose, maltose, and raffinose represented PC1. PC2 was mainly characterised by tyrosine, fructose, sucrose, maltose, and glucose. Separation of the variables was further statistically tested using D_M and Hotelling's T^2 test (Fig. 3D). The D_M between seeds (I) and sprouts (II–IV) showed relative high D_M values, ranging from 113.12 to 408.92. Lower levels of D_M (14.42–20.78) were calculated between the sprout samples. The T^2 results also showed a similar trend with D_M and distinct differences of T^2 values were observed between seeds and sprouts. Sprouts in the control and ATP treated groups exhibited the smallest differences. The F_t and F_c values were checked to verify the separation of the pairwise groups. In the pair of III–IV, the F_t was lower than the F_c value, which indicated the non-significant separation of the two groups in the principal component space.

3.3. Alterative metabolites during energy regulated germination

Based on the PCA results, the supervised data analysis tool OPLS-DA was used in the pairwise groups: mung bean seeds (I) and sprouts in the control (III), sprouts in DNP-treated groups (II) and control (III) groups. The score plot showed that the paired groups I–III and II–III were well separated by PC1 and the goodness of fit parameters R^2 and Q^2 of the two pairs were 0.99 and 0.99, 0.99 and 0.96, respectively (Fig. 4A and C). In addition, the loading S-line helped to discriminate the metabolites of different groups (Fig. 4B and D). Peaks that pointed upwards indicated higher relative contents of a specific metabolite in the second group of a pair group, while the S-line presented a downward trend there was a higher amount of the metabolites in the first group of the pair. According to the results of I–III, the relative contents of metabolites located around 0.5–3.0 ppm showed higher levels in mung bean seed. Also, the downward peaks at around 5.3 ppm indicated higher amounts of oleic acid and linoleic acid. Moreover, most of the peaks from 3.0 to 5.5 ppm, and the peak at 7.32 ppm (assigned as

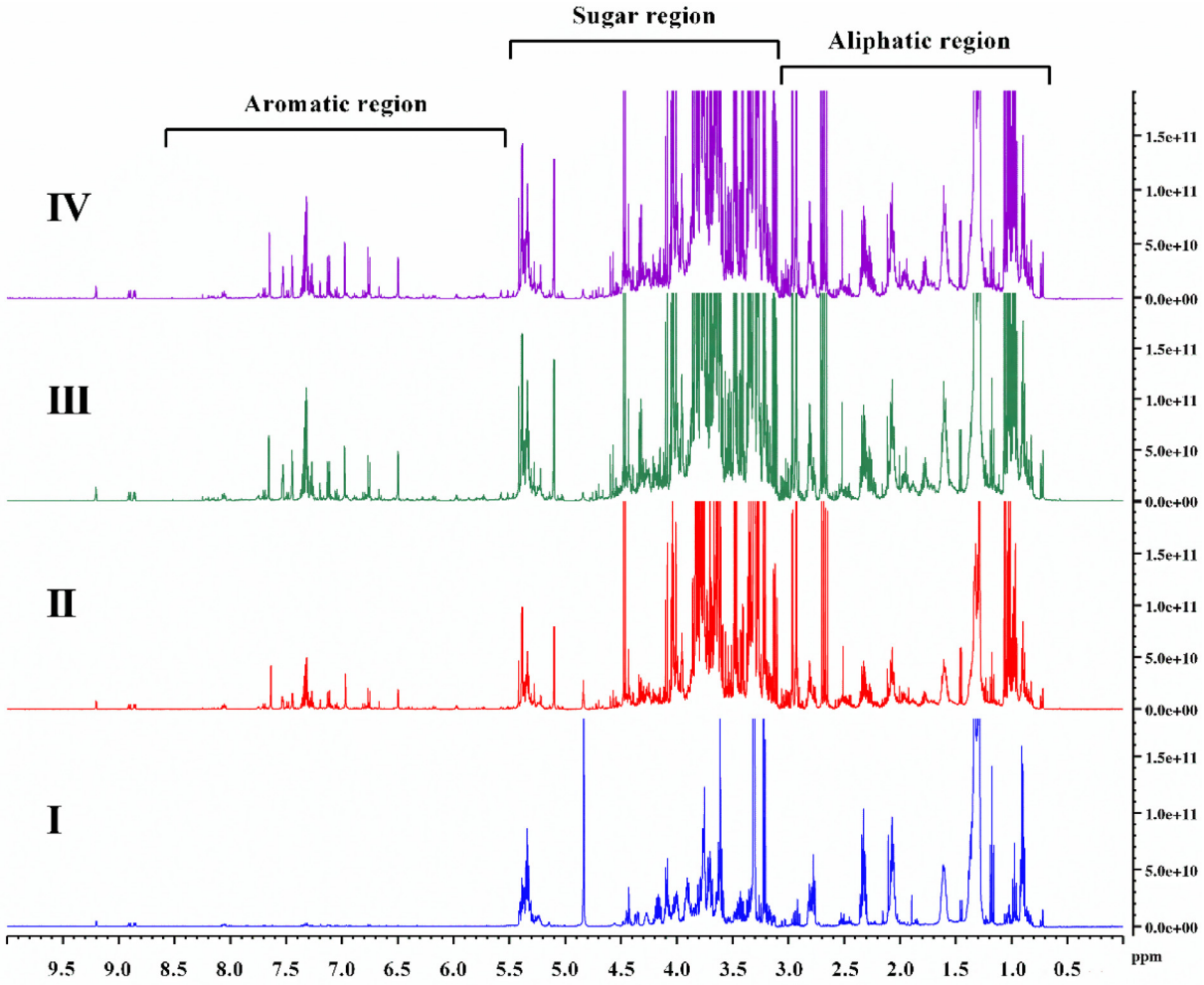

Fig. 1. ^{1}H nuclear magnetic resonance (NMR) spectra of mung beans. Note: group I, rehydrated mung bean seeds at day 0; groups II–IV, mung bean sprouts under 2,4-dinitrophenol (DNP), distilled (DI) water, and ATP treatments, respectively.

phenylalanine), pointed upward, which indicated improved relative contents of the representative metabolites during the germination (Fig. 4B). For the pairwise comparison II–III, the abundant metabolites located in the region of 3.0–5.5 ppm represented higher relative contents in DNP treated sprouts (II). Nevertheless, several peaks that were assigned as glucose, linoleic acid, and oleic acid in this region showed a downward trend. In addition, most of the metabolites in the remaining region also presented higher relative contents in sprouts from the control group (III) (Fig. 4D).

The coefficient plot summarised the changing trends of the identified metabolites in the pairwise groups (Fig. 4E and F). The results showed that after germination and sprouting for 6 days, the levels of raffinose, maltose, glucose, phenylalanine, choline, valine, isoleucine, ascorbic acid, arginine, ketoglutaric acid, acetic acid, *P*-coumaric acid, linolenic acid, 1,3-dihydroxyacetone, histidine, threonine, γ-aminobutyric acid, galactose, vanillin, arabinose, asparagine, and sucrose were increased. By contrast, decreased relative contents of betaine, oleic acid, fructose, linoleic acid, succinic acid, tyrosine, ethanol, glutamine, glycolate, trigonelline, and indole-3-acetic acid were recorded. Moreover, the results of the VIP test showed that changes in certain metabolites, including raffinose, maltose, glucose, phenylalanine, ascorbic acid, betaine, oleic acid, fructose, linoleic acid, succinic acid, tyrosine, and glutamine, were statistically significant (VIP $>$ 1 and $P < 0.05$) to discriminate between the two groups (Fig. 4E).

The coefficient plot of II-III represented the difference of metabolites in the two groups (Fig. 4F). Treatment with the ATP inhibitor (DNP) resulted in higher relative contents of various metabolites, including maltose, fructose, raffinose, tyrosine, sucrose, threonine, ascorbic acid, glutamine, ketoglutaric acid, indole-3-acetic acid, histidine, glycolate, trigonelline, asparagine, vanillin, and arginine. By contrast, metabolites such as glucose, phenylalanine, oleic acid, linoleic acid, isoleucine, ethanol, linolenic acid, galactose, 1,3-dihydroxyacetone, choline, valine, acetic acid, succinic acid, betaine, *P*-coumaric acid, γ-aminobutyric acid, and arabinose had higher levels in the control sprouts. The VIP test further verified that 12 metabolites (maltose, fructose, raffinose, tyrosine, sucrose, threonine, glucose, phenylalanine, oleic acid, linoleic acid, isoleucine, and ethanol) were significant factors for pair-wise discrimination.

3.4. Metabolic pathway analysis

Metabolic pathway analysis was conducted to identify the most relevant pathways that were associated with the energy-regulated germination and sprouting of mung beans. Based on the results of OPLS-DA and VIP tests, the selected metabolites were used to test their involvement in pathways using the combination of network analysis and functional enrichment analysis (Fig. S1, Table S3). The pathways that exhibited false discovery rate $P < 0.05$ were considered as statistically significant metabolic pathways. For the germination and sprouting processes of mung beans, a total of 24 pathways were predicted. Furthermore, eight pathways (nitrogen metabolism; tyrosine metabolism; alanine, aspartate and glutamate metabolism; phenylalanine, tyrosine,

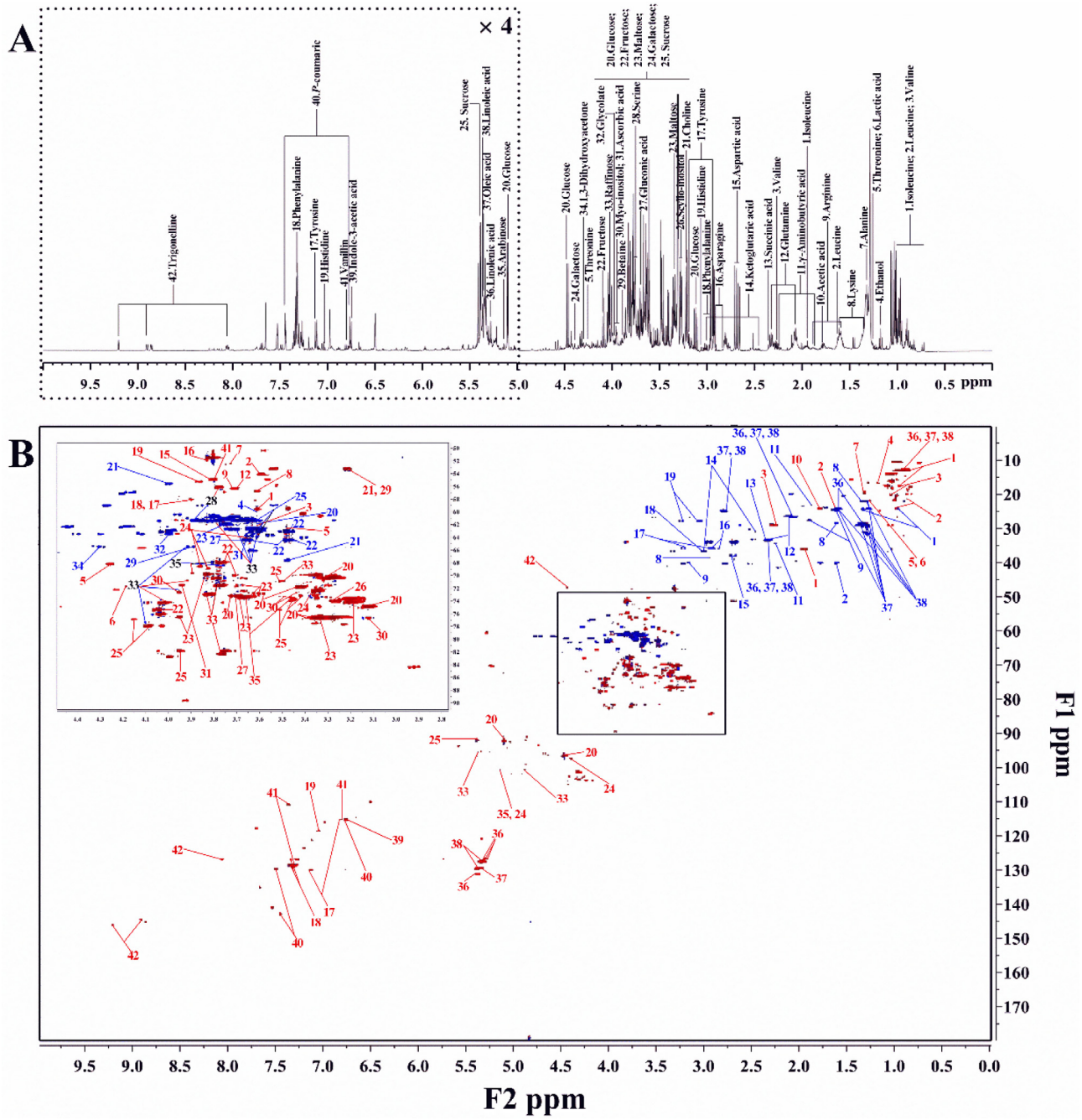

Fig. 2. Representative one-dimensional (1D) ^{1}H nuclear magnetic resonance (NMR) mung bean spectra (A); the corresponding two-dimensional (2D) ^{1}H–^{13}C NMR mung bean spectra. Each number presents a metabolite assigned in the 1D ^{1}H spectra.

and tryptophan biosynthesis; starch and sucrose metabolism; galactose metabolism; aminoacyl-tRNA biosynthesis; and phenylpropanoid biosynthesis) were suggested to be closely related to the biological activity (Fig. S1A and B). Furthermore, the inhibition of ATP production (DNP treatment, II) resulted in notable biological changes in the sprouts. Of the obtained 17 predicted pathways, 6 biological pathways were verified as the key factors that responded to the energy starvation of mung bean sprouts. They were starch and sucrose metabolism; galactose metabolism; aminoacyl-tRNA biosynthesis; phenylalanine, tyrosine, and tryptophan biosynthesis; valine, leucine, and isoleucine biosynthesis; and phenylpropanoid biosynthesis (Fig. S1C and D).

3.5. Expression pattern of selected genes

Fig. 6A shows a heatmap representing the different expression patterns of the glycolysis and TCA cycle related genes. Generally, the relative expression levels of *VrUGPU* and *VrFB* were significantly improved in sprouts compared with those in seeds ($P < 0.05$) (Fig. 6B). After germination and sprouting, the *VrUGPU* level was improved by 67.1% in the control (III). Moreover, DNP treatment (II) resulted in more than four times elevated expression of *VrUGPUs*. For *VrFB*, the expression levels in the control and ATP treated groups (IV) were both notably induced by around 50 times, and the DNP treatment improved the *VrFB* level by 63.2 times. By contrast, the expression levels of *VrPD* in the control and ATP-treated sprouts were downregulated by 41.9% and 47.7%, respectively. Significantly elevated expression of *VrCS* (by

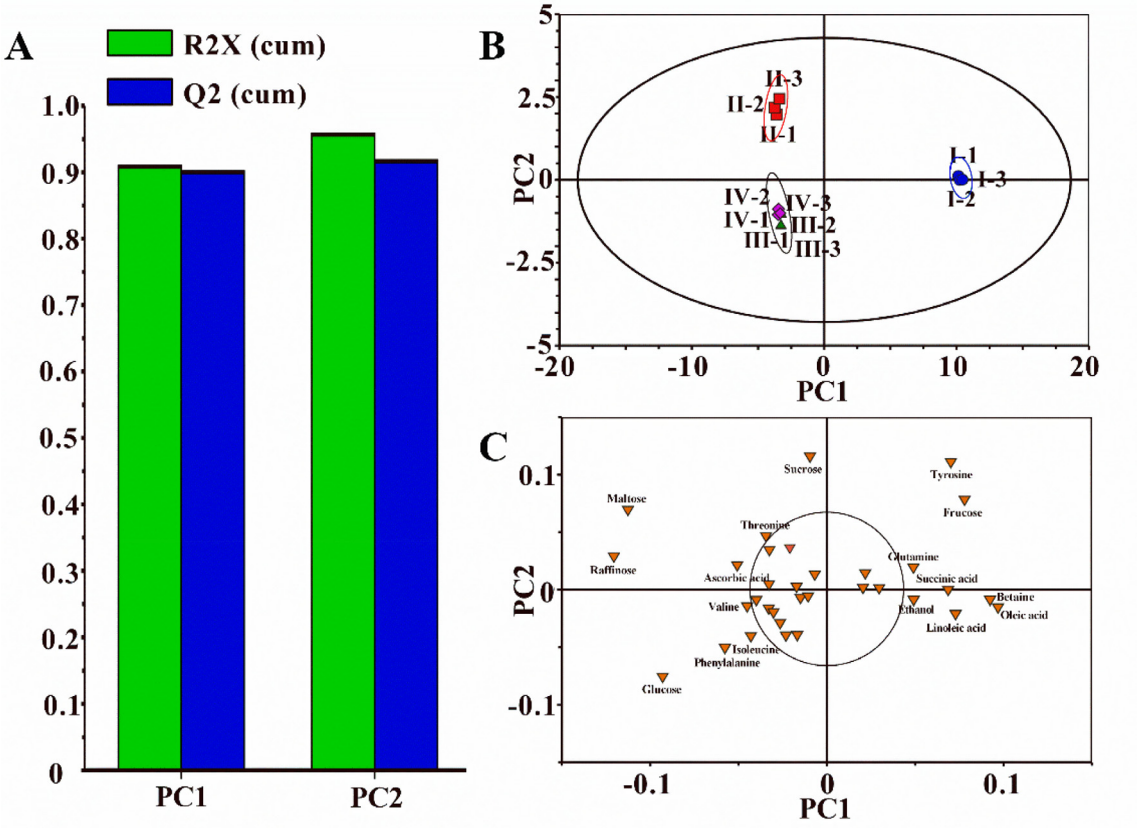

D

Statistical parameter	I-II	I-III	I-IV	II-III	II-IV	III-IV
D_M	408.92	183.18	113.12	20.78	16.96	14.42
T^2	6591.28	6390.92	9088.28	187.41	64.89	2.67
F_c	9.55	9.55	9.55	9.55	9.55	9.55
F_t	9886.91	9586.38	13632.42	281.11	97.33	4.00
Significant status	Yes	Yes	Yes	Yes	Yes	No

Fig. 3. Principal component analysis (PCA) for the metabolite profile of mung bean extracts. The principal components explaining variances used in PCA (A); the score plot of PCA (B); the loading plot of PCA (C); statistical significance analysis of pairwise groups (D). Note: R^2X, explained variable value; Q^2, model predictability value; D_M, Mahalanobis distance; T^2, two-sample Hotelling's T^2 test; F_c, critical F value; F_t, true F value; group I, rehydrated mung bean seeds at day 0; groups II–IV, mung bean sprouts under 2,4-dinitrophenol (DNP), distilled (DI) water, and ATP treatments, respectively.

73.1% compared with seeds) was only observed in DNP-treated sprouts. Moreover, *VrKD* expression was maintained at stable levels in all the tested samples. In addition, the *VrSD* level in the control spouts was notably ($P < 0.05$) reduced by 11.3% and was elevated by around 2-fold under DNP treatment.

4. Discussion

The germination and sprouting of organic edible seeds produce nutritive sprout products that are good alternatives to traditional plant foods (Yu, Li, Ng, Yang, & Wang, 2018; Zhang & Yang, 2017). Recent studies have confirmed the important regulatory role of energy metabolism in the postharvest preservation of fruit and vegetables (Yao, Zhu, Yi, Qu, & Jiang, 2015; Yi et al., 2008). However, little information about the energy-regulated quality formation and physiological activities during the pre-harvest stage is available. Our previous work showed that a positive energy status was a crucial factor to improve the synthesis of nutritive compounds such as phenolics. By contrast, an energy deficit resulted in activation of energy production pathways and suppression of secondary metabolism in broccoli sprouts (Chen, Tan, et al., 2018). In the present study, the overall metabolic changes during the germination and sprouting of mung beans under different energy statuses were evaluated using NMR.

The germination and sprouting processes resulted in dramatic changes in metabolism. The results of ^{1}H spectral analysis showed notable difference between seeds and sprouts (Fig. 1). In mung bean seeds, the ^{1}H signals were mainly located in the region of 0.5–5.5 ppm. Typically, the aliphatic acids and sugars were assigned to this region (Mahmud et al., 2015; Yuan et al., 2017). Further metabolite identification revealed that abundant free amino acids (arginine, glutamine, tyrosine, etc.) existed in mung beans. Moreover, the sugar region (3.0–5.5 ppm) showed multiple saccharide assignments, such as fructose, glucose, and sucrose (Fig. 2, Table S2). Carbohydrates (approximately 62%, w/w) and proteins (approximately 27%, w/w) are the two major components in raw mung bean seeds (Mubarak, 2005). During imbibition, the macromolecules degrade into oligosaccharides and amino acids, which provide nutritive and energy sources for the germination and development processes (Nonogaki, Bassel, & Bewley, 2010; Smiri et al., 2009). In sprouts, the notably higher signal intensities in the sugar region indicated improved soluble sugar contents compared with those in seeds (Fig. 1). These results were consistent with those of a previous study (Wang et al., 2005). Moreover, the peaks

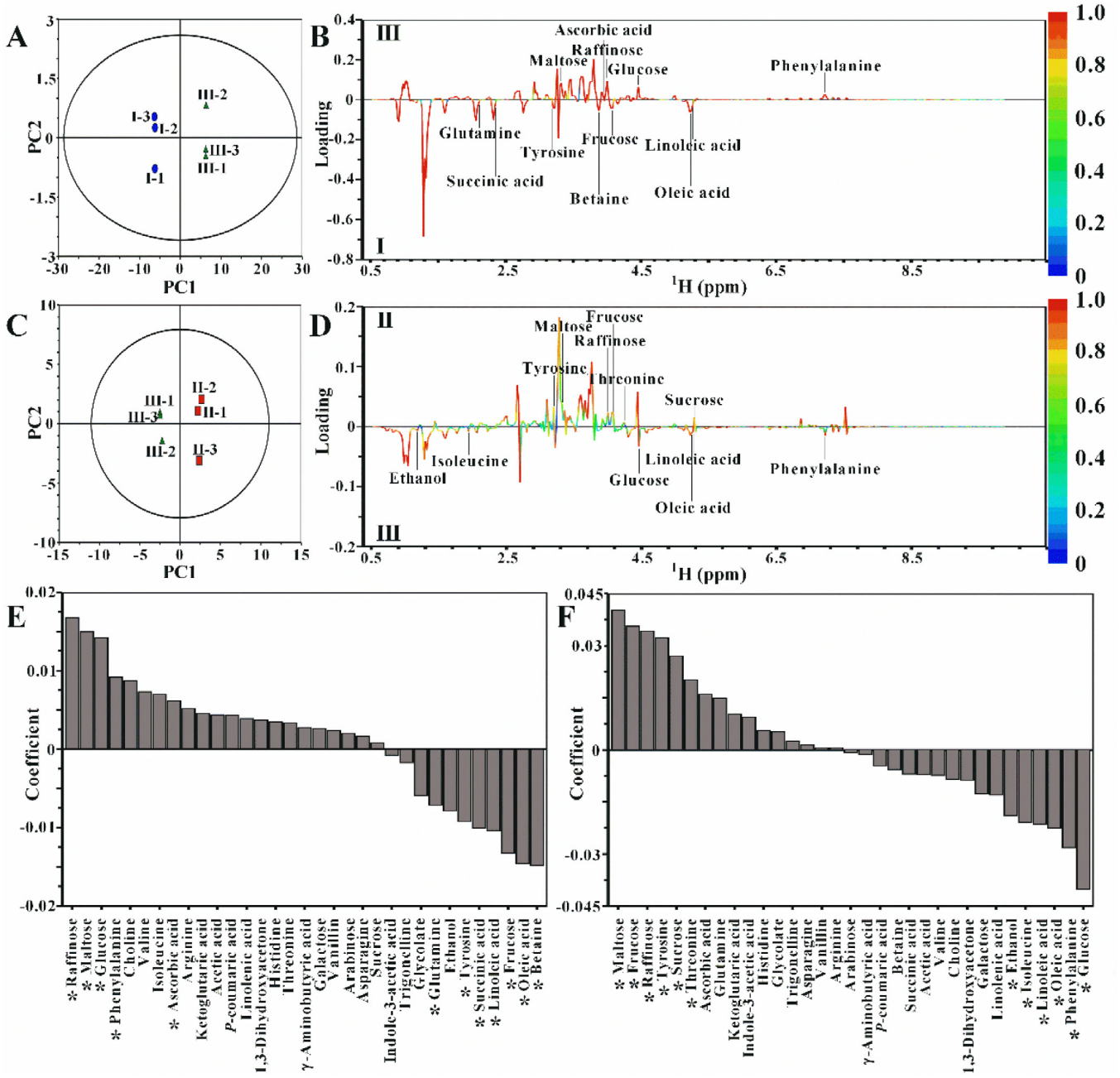

Fig. 4. Orthogonal partial least squares discriminant analysis (OPLS-DA) comparison results of pairwise groups. OPLS-DA score plot of groups I–III, $R^2 = 0.99$, $Q^2 = 0.99$ (A); loading S-line of groups I–III (B); OPLS-DA score plot of groups II–III, $R^2 = 0.99$, $Q^2 = 0.96$ (C); loading S-line of groups II–III (D); coefficient plot of groups I–III (E); coefficient plot of II–III, the metabolites marked with * indicate a significant contribution to the OPLS-DA models (variable importance in projection (VIP) > 1) (F). Note: group I, rehydrated mung bean seeds at day 0; groups II–IV, mung bean sprouts under 2,4-dinitrophenol (DNP), distilled (DI) water, and ATP treatments, respectively. R^2X, explained variable value; Q^2, model predictability value.

in the aromatic region of the ^{1}H NMR spectra indicated the synthesis of phenolics during sprouting (Yuan et al., 2017). Based on further chemical shift analysis, phenolics such as *P*-coumaric acid and vanillin were identified in mung bean sprouts (Fig. 2, Table S2). In plants, phenolic compounds are synthesised to balance the redox equilibrium and to help resist environmental stress, such as pathogen attack (Yeo & Shahidi, 2015; Yi et al., 2010).

PCA is a useful tool to detect the discriminative factors from the high throughput profile (Liu et al., 2018). In this study, the high R^2X and Q^2 values of the PCs indicated the good fitness of the model (Fig. 3A). PC1 explained the majority (90.9%) of the overall data and the opposite PC1 values of sprouts (II, III, and IV) and seeds (I) indicated the dramatic metabolic differences between the two stages (Fig. 3B). In addition, the D_M, T^2, and F_t values between the seeds and sprouts from the three groups showed higher values, which indicated significant separation of the seeds group (Fig. 3D). The D_M and T^2 tests provide convincing quantitative metrics to compare the magnitude of cluster separation (Mahmud, Shrestha, Boroujerdi, & Chowdhury, 2015). Moreover, lower, but still significant, pairwise separations among sprouts (II-III and II-IV) were observed (Fig. 3B and D), indicating the important role of sufficient energy for metabolism. The loading plot that was responsible for the group separation was further evaluated and the results revealed that some unsaturated fatty acids, such as oleic acid and linoleic acid, were closely associated with mung bean seeds. The results were in accordance with those of a previous report (Anwar, Latif, Przybylski, Sultana, & Ashraf, 2007). The lipids in

higher plant seeds are mainly used as energy sources during embryo development (Pujar et al., 2006). Conversely, various saccharides, such as glucose, sucrose, maltose, and raffinose, were characterised in mung bean sprouts. These metabolites are all closely associated with plant energy metabolism (Eveland & Jackson, 2011). The dramatic changes in energy production and consumption between seeds and sprouts contributed to the observed differences in metabolite levels.

OPLS-DA is an extension of supervised partial least squares (PLS) regression. It is widely used to enhance the quality of pairwise classification analysis (Jadhav et al., 2015). The relative high fitness parameters indicated the fit goodness through the well defined separation of I-III and III-II (Fig. 4A and C). The S-line confirmed the higher relative contents of unsaturated fatty acids (oleic and linoleic acids), fructose, and some amino acids in mung bean seeds compared with those in sprouts (Fig. 4B). The results indicated that various pathways might contribute cooperatively to the energy supply during seed germination (Nonogaki et al., 2010; Smiri et al., 2009). Moreover, the red colour of most of the peaks revealed the significant difference in metabolites between the two groups. The S-line between groups II and III indicated that DNP treatment induced the synthesis of saccharides and promoted the consumption and translation of glucose (Fig. 4D). The results indicated that the sugar metabolism related to glycolysis may become the major energy source for mung bean sprouts and that sugar metabolism responded sensitively to the energy starvation status.

Coefficient plots (Fig. 4E and F) were statistically extracted to identify significant metabolites in biochemical pathways (Liu et al., 2018). Of the 33 identified metabolites without overlapping chemical shifts, the relative contents of 22 compounds increased after germination and sprouting. Moreover, the VIP test identified 12 candidate metabolites that might be significantly affected during the complex biological process of germination or sprouting. Accumulated raffinose functions in the transport and storage of carbon, membrane trafficking, mRNA export, and signal transduction. These physiological functions are closely related to seed germination and sprout development (Sengupta, Mukherjee, Basak, & Majumder, 2015). The accumulation of abundant glucose and maltose in mung bean sprouts might be due to the degradation of starch in the endosperm (Kalita, Sarma, & Srivastava, 2017). Moreover, the increase in ascorbic acid helps the sprouts maintain redox equilibrium, and phenylalanine is important for the synthesis of antioxidative phenolics (Wang, Wang, et al., 2016). By contrast, in seeds, the secondary metabolite betaine acts as an important nutrient to regulate the cell osmotic pressure and effectively improve resistance to environmental stresses (Yang et al., 2018). In addition, the higher relative contents of some amino acids (glutamine and tyrosine), lipids (oleic and linoleic acids), and saccharides (fructose) indicated the use of different energy resources in mung bean seeds (Zhao, Zhang, Yan, Qiu, & Baskin, 2018). Succinic acid is an important intermediate product in the TCA cycle and its significantly higher relative contents in seeds indicated higher rates of TCA. These results were in accordance with the results of previous studies in rice seeds during early imbibition (Nonogaki et al., 2010).

Fig. 4F shows that the metabolic changes of mung bean sprouts under DNP resulted in energy starvation. Certain saccharides (maltose, fructose, raffinose, and sucrose) and amino acids (tyrosine and threonine) were induced by DNP treatment. Our previous studies showed that the energy balance of sprouts was maintained by the feedback regulation of the SnRK pathway and that energy deficit activated the ATP synthesis pathway (Chen, Tan, et al., 2018). Thus, the massive synthesis of saccharides may be stimulated by the ATP synthesis system. In addition, lower contents of phenylalanine in DNP-treated sprouts resulted in lower contents of phenolics, such as *P*-coumaric acid, because phenylalanine is the precursor of many phenolics (Wang, Wu, et al., 2016). This result was also consistent with our previous report that DNP treatment reduced the phenolic contents of sprouts (Chen, Zhou, et al., 2018).

The metabolic pathway analysis demonstrated that 24 pathways were associated with the germination and sprouting of mung bean seeds (Fig. S1A and B). Nitrogen metabolism was recognised as the most affected pathway. Indeed, nitrogen metabolism is one of the major metabolism pathways that activate and control the germination and sprouting processes (Osuna, Prieto, & Aguilar, 2015). The various ammonium-based metabolites or molecules provide developmental material and signal transmission factors. The related synthesis, transformation, and degradation of proteins and amino acids are crucial physiological activities for plant development. Another class of vital metabolism in mung bean germination and sprouting is sugar metabolism (Fig. S1A and B). Starch, sucrose, and galactose metabolisms participate in the germination and sprouting processes. These sugar molecules act as energy sources, signal transduction factors, and in phytohormone and stress responses during germination (Rolland, Baena-Gonzalez, & Sheen, 2006). Moreover, crosstalk between nitrogen and sugar metabolism helps to maintain the C/N balance and further affect the germination and sprouting processes (Osuna et al., 2015).

The reprograming of metabolic pathways of mung bean sprouts under energy deficit is shown in Fig. S1C and D. Similar to the results of PCA, sugar metabolism was significantly affected by DNP treatment. Energy starvation activated sugar metabolism and increased the contents of related saccharides. Among sugars, glucose plays a critical role in sugar metabolism, and the activation of sugar metabolism resulted in decreased relative contents of glucose due to its consumption and transformation. In addition, some amino acid metabolisms were affected by DNP treatment. Amino acid metabolisms are regulated or participated in energy metabolism in plants. For example, the oxidation of tyrosine yields 34 molecules of ATP, which is comparable to that gained by glucose oxidation. Also, glutamine can be converted into γ-aminobutyric acid and then transformed into succinic acid to participate in the TCA cycle (Hildebrandt, Nesi, Araújo, & Braun, 2015). Moreover, the activation of aminoacyl-tRNA biosynthesis in energy regulated germination and sprouting of mung beans indicated that abundant protein or amino acid translation events occurred in these physiological processes (Moore, Gossmann, & Dietz, 2016).

The main pathways affected during energy-regulated germination are summarised and illustrated in Fig. 5, based on the KEGG database and MetaboAnalyst 4.0. Metabolites in red refer to increased relative concentrations and metabolites coloured green refer to decreased contents. In summary, during the germination of mung beans, dramatic metabolic changes occurred (Fig. 5A). The mung bean seeds used different energy resources (saccharides, lipids, and amino acids) for these physiological activities. The TCA cycle was strongly induced after rehydration for 12 h. The amino acids (glutamine and tyrosine) that participate in the TCA cycle had higher levels in seeds. After germination and sprouting for 6 days, sugar metabolism was significantly activated and the related sugars (maltose, glucose and raffinose) accumulated in mung bean sprouts. Glycolysis may become the major energy source of the sprouted plants. Furthermore, secondary metabolites, such as ascorbic acid, were synthesized. The amount of the intermediate metabolite (phenylalanine) of phenolics also increased. Along with growth and division, the nutritive values of mung beans were enhanced. The alteration of energy sources and synthesis of bioactive compounds were the major variations during the germination of mung beans.

The reprograming mechanism of mung bean sprouts under energy deficit was also studied (Fig. 5B). DNP caused energy starvation and significantly activated sugar metabolism. Glucose was massively consumed and transformed into other saccharides. The block in ATP production caused the relative contents of amino acids that participate in the TCA cycle to increase. By contrast, the production of secondary metabolites or related intermediate metabolites was inhibited when energy was insufficient. However, the TCA cycle was not significantly affected at this stage. These results indicated that complex biological changes occurred during the germination and sprouting of mung beans, and that their nutritive values increased. Energy status is a crucial

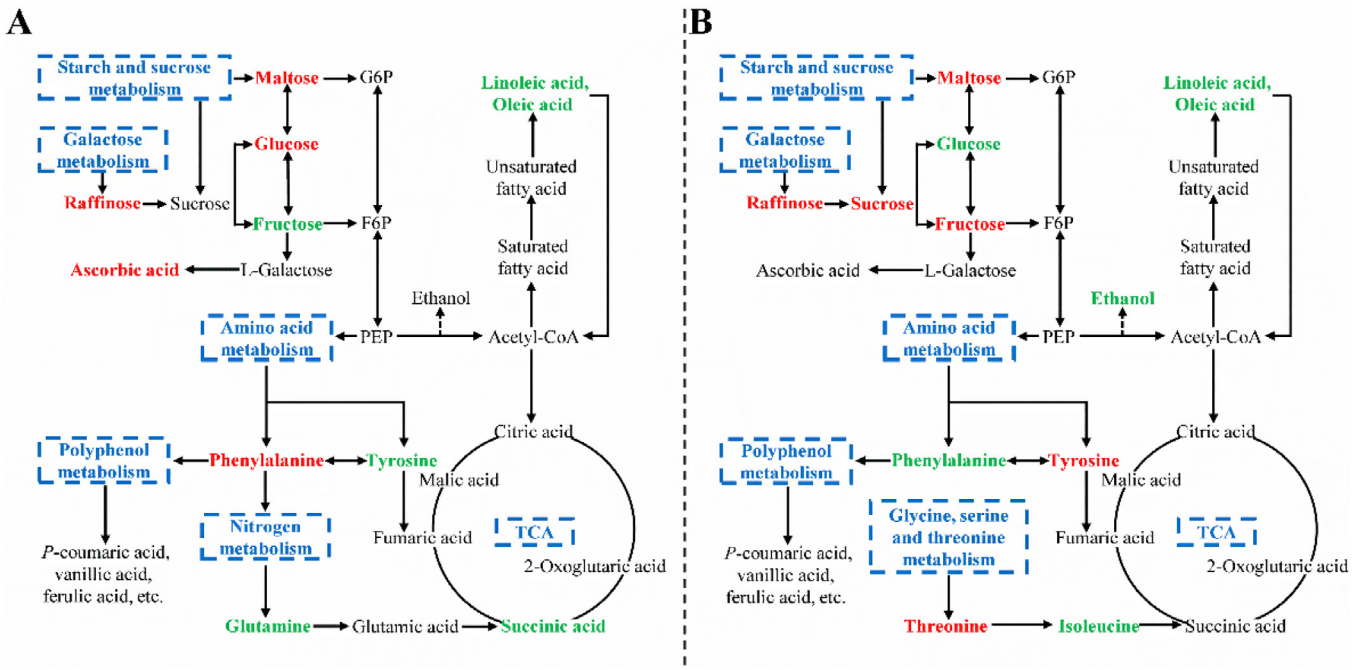

Fig. 5. Biochemical pathway analysis for the germination and sprouting processes of mung beans (A) and reprogramming of metabolic pathways of mung bean sprouts under energy deficit (B). Metabolites coloured in red and green represent higher and lower relative contents, respectively. Note: G6P, glucose-6-phosphate; F6P, fructose-6-phospate; PEP, phosphoenolpyruvate; TCA, tricarboxylic acid. (For interpretation of the references to colour in this figure legend, the reader is referred to the web version of this article.)

factor for the physiological process involved in development and nutritive synthesis. This overall metabolic analysis helps to clarify the underling mechanism of germination and sprouting, and provides a reference for the further regulation and production of higher quality vegetables.

To further understand and confirm the summarised metabolic mechanism, the expression of several genes related to glycolysis and the TCA cycle were tested using qPCR. UGPU synthesises UDP-glucose from glucose-1-phosphate and plays a key role in glycogenesis and cell wall synthesis. FB is an enzyme that converts fructose-1,6-bisphosphate to fructose 6-phosphate, which then participates in the gluconeogenesis and TCA cycles. Furthermore, PD contributes to the transformation of pyruvate to acetyl-CoA. In addition, the TCA cycle related enzymes CS, KD, and SD are responsible for the synthesis of citric acid and the degradation of 2-oxoglutaric acid and succinic acid, respectively (Avin-Wittenberg et al., 2012). The qPCR results showed that compared with seeds (I), sprouts (II–IV) exhibited higher expression levels of *VrUGPU* and *VrFB* (Fig. 6). Therefore, sugar metabolism was activated in sprouts at the transcriptional level. In addition, the TCA cycle related genes in sprouts were maintained at similar levels or even decreased. Among sprouts groups, there were almost no significant differences between the control (III) and ATP (II) treated groups. However, DNP treatment induced higher expression levels of most of the selected genes compared with those in the other groups. Thus, the transcriptional results were generally in accordance with our metabolic hypothesis of energy regulated germination and sprouting of mung beans.

5. Conclusion

The metabolomic analysis of energy-regulated germination and sprouting of mung beans was studied using NMR spectroscopy. The obtained spectral and statistical results indicated that dramatic metabolic changes occurred during mung bean development. In addition, sufficient energy supply was crucial for the nutritive quality and metabolism of mung bean sprouts. The PCA and OPLS-DA analyses identified significant differences among rehydrated seeds, sprouts in control group, and sprouts developed under DNP treatment, which resulted in an energy deficit. Among the 42 identified compounds, oleic acid, linoleic acid, and succinic acid were associated with seeds, while other metabolites including sucrose, maltose and glucose were closely related to sprouts. Furthermore, nitrogen, sugar, and amino acid metabolic pathways were mainly associated with the germination of mung beans. By contrast, sugar metabolism was activated by DNP to reprogramme the energy balance. The expression patterns of glycolysis and TCA cycle-related genes were in accord with the NMR metabolic study. The transcriptional results further verified the metabolic hypothesis. The present study showed that NMR-based metabolomics is a useful method to identify the key metabolites in energy-regulated germination and sprouting processes of mung beans. These results provide insights to understand the metabolic mechanism of sprout germination and help to actively control the development process and improve the quality of mung beans.

Acknowledgement

This study was supported by the Singapore Ministry of Education Academic Research Fund Tier 1 (R-143-000-A40-114), projects 31371851 and 31071617 supported by NSFC, Natural Science Foundation of Jiangsu Province (BK20181184) and an industry grant from Funlife Food Industry (Chongqing) Co., Ltd (R-143-000-673-597).

Conflict of interest

We declare that we do not have any commercial or associative interest that represents a conflict of interest in connection with this manuscript. We have no financial and personal relationships with other people or organisations that can inappropriately influence our work.

Appendix A. Supplementary material

Supplementary data to this article can be found online at https://doi.org/10.1016/j.foodchem.2019.01.183.

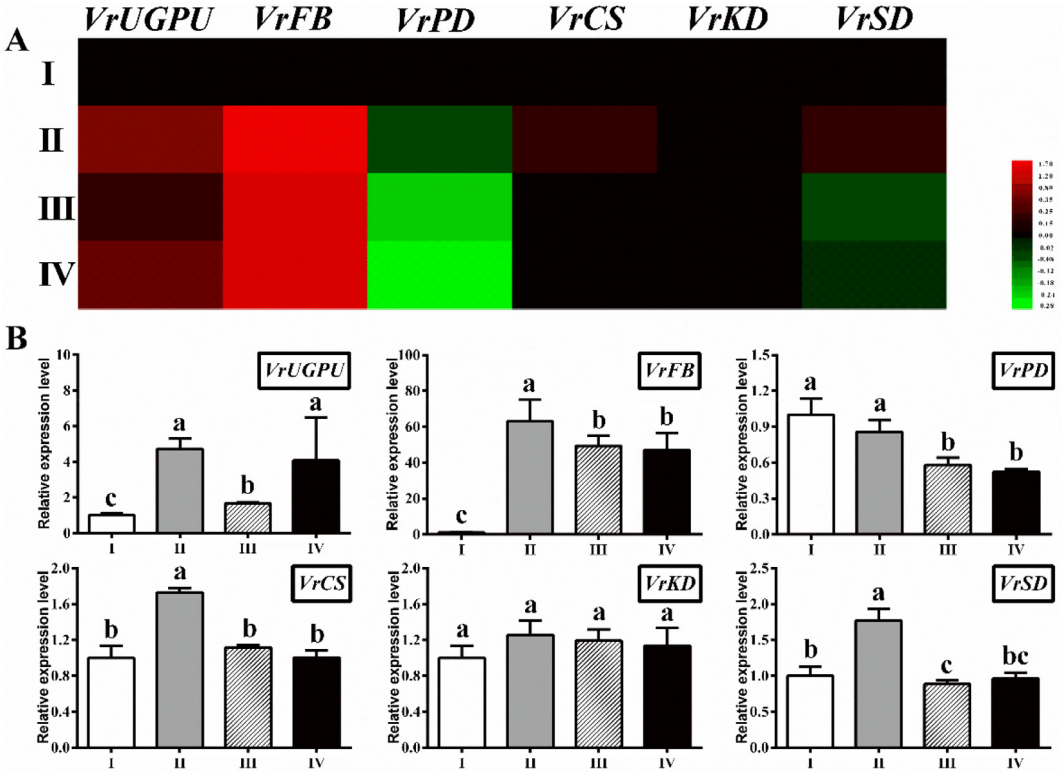

Fig. 6. Heatmap of glycolysis and TCA cycle-related genes in mung bean. Levels of downregulated expression (green) or upregulated expression (red) are shown on a log10 scale for each gene (n = 3) (A); Relative expression levels of glycolysis and TCA cycle-related genes in mung bean (B). Note: UGPU, UTP-glucose-1-phosphate uridylyltransferase; FB, fructose-1,6-bisphosphatase; PD, pyruvate dehydrogenase; CS, citrate synthase; KD, 2-ketoglutarate dehydrogenase; SD, succinate dehydrogenase; group I, rehydrated mung bean seeds at day 0; groups II–IV, mung bean sprouts under 2,4-dinitrophenol (DNP), distilled (DI) water, and ATP treatments, respectively. (For interpretation of the references to colour in this figure legend, the reader is referred to the web version of this article.)

References

Aguilera, Y., Díaz, M. F., Jiménez, T., Benítez, V., Herrera, T., Cuadrado, C., ... Martín-Cabrejas, M. A. (2013). Changes in nonnutritional factors and antioxidant activity during germination of nonconventional legumes. *Journal of Agricultural and Food Chemistry, 61*(34), 8120–8125.

Anwar, F., Latif, S., Przybylski, R., Sultana, B., & Ashraf, M. (2007). Chemical composition and antioxidant activity of seeds of different cultivars of mungbean. *Journal of Food Science, 72*(7), S503–S510.

Avin-Wittenberg, T., Tzin, V., Angelovici, R., Less, H., & Galili, G. (2012). Deciphering energy-associated gene networks operating in the response of *Arabidopsis* plants to stress and nutritional cues. *The Plant Journal, 70*(6), 954–966.

Baenas, N., García-Viguera, C., & Moreno, D. A. (2014). Biotic elicitors effectively increase the glucosinolates content in *Brassicaceae* sprouts. *Journal of Agricultural and Food Chemistry, 62*(8), 1881–1889.

Chen, L., Tan, G. J. T., Pang, X., Yuan, W., Lai, S., & Yang, H. (2018a). Energy regulated nutritive and antioxidant properties during the germination and sprouting of broccoli sprouts (*Brassica oleracea* var. *italica*). *Journal of Agricultural and Food Chemistry, 66*(27), 6975–6985.

Chen, L., Zhou, Y., He, Z., Liu, Q., Lai, S., & Yang, H. (2018b). Effect of exogenous ATP on the postharvest properties and pectin degradation of mung bean sprouts (*Vigna radiata*). *Food Chemistry, 251*, 9–17.

Duenas, M., Hernández, T., Estrella, I., & Fernández, D. (2009). Germination as a process to increase the polyphenol content and antioxidant activity of lupin seeds (*Lupinus angustifolius* L.). *Food Chemistry, 117*(4), 599–607.

Eveland, A. L., & Jackson, D. P. (2011). Sugars, signalling, and plant development. *Journal of Experimental Botany, 63*(9), 3367–3377.

Hildebrandt, T. M., Nesi, A. N., Araújo, W. L., & Braun, H. P. (2015). Amino acid catabolism in plants. *Molecular Plant, 8*(11), 1563–1579.

Jadhav, S., Gulati, V., Fox, E. M., Karpe, A., Beale, D. J., Sevior, D., ... Palombo, E. A. (2015). Rapid identification and source-tracking of *Listeria monocytogenes* using MALDI-TOF mass spectrometry. *International Journal of Food Microbiology, 202*, 1–9.

Kalita, D., Sarma, B., & Srivastava, B. (2017). Influence of germination conditions on malting potential of low and normal amylose paddy and changes in enzymatic activity and physico chemical properties. *Food Chemistry, 220*, 67–75.

Liu, Q., Wu, J. E., Lim, Z. Y., Aggarwal, A., Yang, H., & Wang, S. (2017b). Evaluation of the metabolic response of *Escherichia coli* to electrolysed water by ^{1}H NMR spectroscopy. *LWT-Food Science and Technology, 79*, 428–436.

Liu, Q., Wu, J. E., Lim, Z. Y., Lai, S., Lee, N., & Yang, H. (2018). Metabolite profiling of *Listeria innocua* for unravelling the inactivation mechanism of electrolysed water by nuclear magnetic resonance spectroscopy. *International Journal of Food Microbiology, 271*, 24–32.

Liu, J., Yuan, Y., Wu, Q., Zhao, Y., Jiang, Y., John, A., ... Yang, B. (2017a). Analyses of quality and metabolites levels of okra during postharvest senescence by ^{1}H-high resolution NMR. *Postharvest Biology and Technology, 132*, 171–178.

Mahmud, I., Kousik, C., Hassell, R., Chowdhury, K., & Boroujerdi, A. F. (2015). NMR spectroscopy identifies metabolites translocated from powdery mildew resistant rootstocks to susceptible watermelon scions. *Journal of Agricultural and Food Chemistry, 63*(36), 8083–8091.

Mahmud, I., Shrestha, B., Boroujerdi, A., & Chowdhury, K. (2015). NMR-based metabolomics profile comparisons to distinguish between embryogenic and non-embryogenic callus tissue of sugarcane at the biochemical level. *Vitro Cellular & Developmental Biology-plant, 51*(3), 340–349.

Moore, M., Gossmann, N., & Dietz, K.-J. (2016). Redox regulation of cytosolic translation in plants. *Trends in Plant Science, 21*(5), 388–397.

Mubarak, A. (2005). Nutritional composition and antinutritional factors of mung bean seeds (*Phaseolus aureus*) as affected by some home traditional processes. *Food Chemistry, 89*(4), 489–495.

Nonogaki, H., Bassel, G. W., & Bewley, J. D. (2010). Germination—Still a mystery. *Plant Science, 179*(6), 574–581.

Osuna, D., Prieto, P., & Aguilar, M. (2015). Control of seed germination and plant development by carbon and nitrogen availability. *Frontiers in Plant Science, 6*, 1023.

Pujar, A., Jaiswal, P., Kellogg, E. A., Ilic, K., Vincent, L., Avraham, S., ... Rhee, S. Y. (2006). Whole-plant growth stage ontology for angiosperms and its application in plant biology. *Plant Physiology, 142*(2), 414–428.

Rolland, F., Baena-Gonzalez, E., & Sheen, J. (2006). Sugar sensing and signaling in plants: Conserved and novel mechanisms. *Annual Review of Plant Biology, 57*, 675–709.

Sengupta, S., Mukherjee, S., Basak, P., & Majumder, A. L. (2015). Significance of galactinol and raffinose family oligosaccharide synthesis in plants. *Frontiers in Plant Science, 6*, 656.

Smiri, M., Chaoui, A., & El Ferjani, E. (2009). Respiratory metabolism in the embryonic axis of germinating pea seed exposed to cadmium. *Journal of Plant Physiology, 166*(3), 259–269.

Tang, D., Dong, Y., Ren, H., Li, L., & He, C. (2014). A review of phytochemistry, metabolite changes, and medicinal uses of the common food mung bean and its sprouts (*Vigna radiata*). *Chemistry Central Journal, 8*(1), 4.

Vong, W. C., Hua, X. Y., & Liu, S. Q. (2018). Solid-state fermentation with *Rhizopus oligosporus* and *Yarrowia lipolytica* improved nutritional and flavour properties of okara. *LWT-Food Science and Technology, 90*, 316–322.

Wang, K., Lai, Y., Chang, J., Ko, T. F., Shyu, S. L., & Chiou, R. Y. Y. (2005). Germination of peanut kernels to enhance resveratrol biosynthesis and prepare sprouts as a functional vegetable. *Journal of Agricultural and Food Chemistry, 53*(2), 242–246.

Wang, H., Qian, Z., Ma, S., Zhou, Y., Patrick, J. W., Duan, X., ... Qu, H. (2013). Energy status of ripening and postharvest senescent fruit of litchi (*Litchi chinensis* Sonn.). *BMC Plant Biology, 13*(1), 55.

Wang, H., Wang, J., Guo, X., Brennan, C. S., Li, T., Fu, X., ... Liu, R. H. (2016b). Effect of germination on lignan biosynthesis, and antioxidant and antiproliferative activities in flaxseed (*Linum usitatissimum* L.). *Food Chemistry, 205*, 170–177.

Wang, G., Wu, L., Zhang, H., Wu, W., Zhang, M., Li, X., & Wu, H. (2016a). Regulation of the phenylpropanoid pathway: A mechanism of selenium tolerance in peanut (*Arachis hypogaea* L.) seedlings. *Journal of Agricultural and Food Chemistry, 64*(18), 3626–3635.

Yang, S., Zhao, N., Yang, Y., Hu, Y., Dong, H., & Zhao, R. (2018). Mitotically stable modification of DNA methylation in IGF2/H19 imprinting control region is associated with activated hepatic IGF2 expression in offspring rats from betaine-supplemented dams. *Journal of Agricultural and Food Chemistry, 66*(11), 2704–2713.

Yao, F., Zhu, H., Yi, C., Qu, H., & Jiang, Y. (2015). MicroRNAs and targets in senescent litchi fruit during ambient storage and post-cold storage shelf life. *BMC Plant Biology, 15*(1), 181.

Yeo, J., & Shahidi, F. (2015). Critical evaluation of changes in the ratio of insoluble bound to soluble phenolics on antioxidant activity of lentils during germination. *Journal of Agricultural and Food Chemistry, 63*(2), 379–381.

Yi, C., Jiang, Y., Shi, J., Qu, H., Xue, S., Duan, X., ... Prasad, N. K. (2010). ATP-regulation of antioxidant properties and phenolics in litchi fruit during browning and pathogen infection process. *Food Chemistry, 118*(1), 42–47.

Yi, C., Qu, H., Jiang, Y., Shi, J., Duan, X., Joyce, D., & Li, Y. (2008). ATP-induced changes in energy status and membrane integrity of harvested litchi fruit and its relation to pathogen resistance. *Journal of Phytopathology, 156*(6), 365–371.

Yu, X., Li, Y., Ng, M., Yang, H., & Wang, S. (2018). Comparative study of pyrethroids residue in fruit peels and fleshes using polystyrene-coated magnetic nanoparticles based clean-up techniques. *Food Control, 85*, 300–307.

Yuan, Y., Zhao, Y., Yang, J., Jiang, Y., Lu, F., Jia, Y., & Yang, B. (2017). Metabolomic analyses of banana during postharvest senescence by ^{1}H-high resolution-NMR. *Food Chemistry, 218*, 406–412.

Zhang, J., & Yang, H. (2017). Effects of potential organic compatible sanitisers on organic and conventional fresh-cut lettuce (*Lactuca sativa* Var. *Crispa* L). *Food Control, 72*, 20–26.

Zhang, N., Zhang, H.-J., Sun, Q.-Q., Cao, Y.-Y., Li, X., Zhao, B., ... Guo, Y.-D. (2017). Proteomic analysis reveals a role of melatonin in promoting cucumber seed germination under high salinity by regulating energy production. *Scientific Reports, 7*(1), 503.

Zhao, M., Zhang, H., Yan, H., Qiu, L., & Baskin, C. C. (2018). Mobilization and role of starch, protein, and fat reserves during seed germination of six wild grassland species. *Frontiers in Plant Science, 9*, 234.